



Annealing effects on microstructure and mechanical properties of cryorolled Fe-25Cr-20Ni steel

Yi Xiong^{a,b,*}, Tiantian He^c, Huipeng Li^a, Yan Lu^a, Fengzhang Ren^{a,b}, Alex A. Volinsky^d

^a School of Materials Science and Engineering, Henan University of Science and Technology, Luoyang 471023, China

^b Collaborative Innovation Center of Nonferrous Metals, Luoyang 471023, China

^c National United Engineering Laboratory for Advanced Bearing Tribology, Henan University of Science and Technology, Luoyang 471023, China

^d Department of Mechanical Engineering, University of South Florida, Tampa, FL 33620, USA

ARTICLE INFO

Keywords:

Cryorolling
Annealing
Ultrafine-grained austenitic stainless steel
Microstructure
Mechanical properties

ABSTRACT

Annealing effects on microstructure and mechanical properties of the cryorolled Fe-25Cr-20Ni austenitic stainless steel were investigated by means of optical, scanning and transmission electron microscopy, X-ray diffraction, microhardness and mini-tensile testing. After 90% cryorolling, the grains of austenitic stainless steel were refined to the nanometer scale, and the nano-level grain size increased to the submicron scale after subsequent annealing. The recrystallization temperature of the cryorolled Fe-25Cr-20Ni steel was about 730 °C. After annealing for 10 min at 800 °C, the microstructure was fully recrystallized, and the grain size was about 500 nm. The growth of recrystallization grains occurred with further annealing temperature increase. After annealing for 10 min at 1000 °C, the grain size increased to about 2 μm. Meanwhile, the elongation was nearly the same as the original un-deformed sample, but the yield strength and tensile strength is 2.3 and 1.5 times of the original un-deformed sample, and the toughness increased by 27%. Tensile fracture morphology changed from a mixture of quasi-cleavage and ductile fracture (before annealing) to typical ductile fracture (after annealing).

1. Introduction

Grain refinement can increase metals strength, as it improves toughness. Therefore, grain refinement has been attracting considerable leaning from material engineering science [1]. In recent years, there has been an interest in developing nano/ultrafine grain metal materials to get high strength/good ductility alloys. For this purpose, several techniques including severe plastic deformation [2–4] and advanced thermo-mechanical processes [5,6] have been used. Austenitic stainless steels are widely used in chemical and petrochemical industry due to their excellent toughness, plasticity and corrosion resistance. Since austenitic stainless steels have relatively low strength, it is difficult to use them as structural materials. Due to the single phase austenite, phase transformation does not take place during heating or cooling processes. Thus, the austenitic stainless steels are often refined by severe plastic deformation. At present, ultrafine-grained austenitic stainless steels are produced by equal channel angular pressing (ECAP) [7], accumulative rolling [8], cold rolling [9], cryorolling [10], subsequent annealing and cyclic thermal processing [11]. Recent studies focus on austenitic stainless steels with the occurrence of martensitic transformation during deformation. Huang et al. [7] found that the

304L austenitic stainless steel was refined due to the occurrence of martensitic transformation induced by ECAP. Shen et al. [12] obtained the 304 austenitic stainless steel with grain size of about 270 nm and tensile strength of 2 GPa prepared by accumulative rolling and short time annealing. According to Shakhova et al. [13], martensitic transformation occurred in 316 and 304 austenitic stainless steels after cold rolling, and the subsequent high temperature annealing lead to the reversal transformation of deformation-induced martensite, which caused austenitic grain refinement. Ma et al. [14] reported that severe cold rolling in the range of 75–90% introduces 200–300 nm α' -lath martensite in 304L stainless steels, which finally recrystallized into 300 nm size γ -grain upon reversed annealing at 640 °C for 10 min, resulting in the yield strength improvement from 120 MPa to 708 MPa without loss of macroscopic plasticity. Wu et al. [15] also showed that the ultrafine-grained 316L austenitic stainless steel was prepared by cold rolling and annealing. In their studies, the austenitic grain size distribution was bimodal and the source of the bimodal distribution was discussed. However, there are only a few reports dealing with the grain refinement of austenitic stainless steels with no martensitic transformation during deformation.

Compared with traditional room temperature rolling, cryorolling

* Corresponding author at: School of Materials Science and Engineering, Henan University of Science and Technology, Luoyang 471023, China.
E-mail address: xiongy@haust.edu.cn (Y. Xiong).

can effectively suppress dynamic recovery, improve distributed uniformity of the structure, and refine the grain size [16,17]. To date, cryorolling and annealing have been applied by many researchers for producing ultrafine-grained Al, Cu, Mg and their alloys with the aim of increasing strength [18–21]. However, the reports of cryorolling and annealing are limited for the nonferrous metals and only a few studies [10] are devoted to the microstructure and mechanical properties of ferrous metals after cryorolling and annealing. In our previous work [22], microstructure and mechanical properties of the Fe-25Cr-20Ni austenitic stainless steel after cryorolling with different reductions were investigated. When the cryorolling was 90%, the grain size was refined to the nanometer scale. The microhardness and the strength of the austenitic stainless steel increased with the rolling deformation, while, the corresponding elongation decreased sharply. In order to obtain the austenitic stainless steel with excellent comprehensive mechanical properties, in the present paper, microstructure and mechanical properties of the Fe-25Cr-20Ni austenitic stainless steel are studied by cryorolling with 90% deformation and subsequent annealing at different temperatures. The results discussed in this paper can provide useful experimental support for development and applications of ultrafine-grained austenitic stainless steels.

2. Materials and experimental procedure

2.1. Materials

Vacuum induction furnace was used to manufacture the investigated 150 kg steel ingot with the following chemical composition (in wt%): 0.06 C, 0.3Si, 0.6Mn, 0.02 P, 0.005 S, 25Cr, 20Ni, 0.25N, 0.5Nb and balance Fe. After the electro-slag remelting (ESR) process, the 150 kg ingot was hot forged down to a 5 mm thick slab. The samples were then cryorolled in the strain rate range of $\dot{\epsilon} = 0.6\text{--}1.5\text{ s}^{-1}$ from 5 to 0.5 mm thickness, i.e. an accumulated strain of $\epsilon = 2.32$, with a reduction of $\sim 5\%$ per pass. Cryorolling was performed by immersing the samples into liquid nitrogen for 10–15 min before and after each rolling pass, and liquid nitrogen was sprayed on the surface of rollers and samples. The cryorolling temperature ranged from $-130\text{ }^{\circ}\text{C}$ to $-90\text{ }^{\circ}\text{C}$. A sketch map of the cryorolling process was shown in Fig. 1. The samples after cryorolling were annealed at $500\text{ }^{\circ}\text{C}$, $600\text{ }^{\circ}\text{C}$, $700\text{ }^{\circ}\text{C}$, $800\text{ }^{\circ}\text{C}$, $900\text{ }^{\circ}\text{C}$ and $1000\text{ }^{\circ}\text{C}$, respectively. The holding time was 10 min, which was chosen based on the Etienne et al. study [4]. Then the samples were air-cooled to room temperature. In order to determine the recrystallization temperature of the Fe-25Cr-20Ni steel after 90% cryorolling, annealing temperatures of $730\text{ }^{\circ}\text{C}$, $750\text{ }^{\circ}\text{C}$ and $770\text{ }^{\circ}\text{C}$ were selected with the holding time of 10 min.

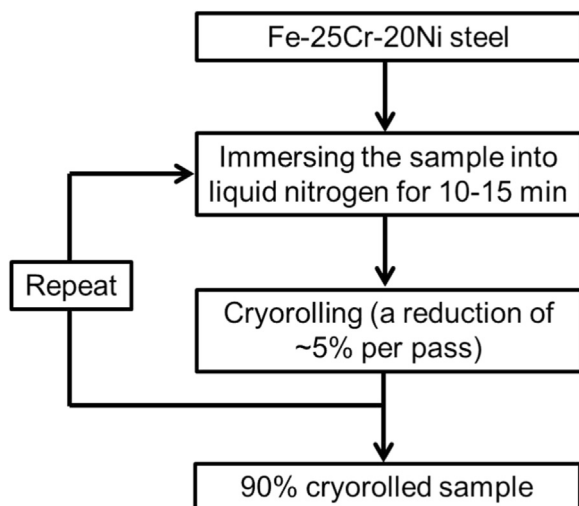


Fig. 1. A sketch map of the cryorolling process.

2.2. Experimental procedure

Microstructure characterization was carried out using optical microscopy (OLYMPUS PMG3) and transmission electron microscopy (TEM, JEM-2010). For metallographic examination, samples were prepared by electrolytic etching using chromic acid solution with 3 V applied voltage. For the TEM study, mechanically thinned 50 μm discs were prepared using twin gun precision ion polishing system (Gatan, model 691). The operating voltage of TEM was 200 kV. X-ray diffraction (XRD) experiments were carried out using the D8ADVANCE X-ray diffractometer. The tube voltage and current were 35 kV and 40 mA, respectively. The tube anode was $\text{CuK}\alpha_1$ ($\lambda = 0.15406\text{ nm}$), and the X-ray beam diameter was about 2 mm. The scan rate was $0.02^{\circ}/\text{s}$ with 1 s per step. The dislocation density was estimated by the W-H method [23]. Microhardness was measured using the MH-3 Vickers microhardness tester with 200 g normal load and 10 s holding time on the as-polished regions. An average microhardness value was determined based on 5 indentation measurements. Mini-tensile test specimens with a gage length of 10 mm, 2.5 mm wide and 0.51 mm thick were prepared along the longitudinal direction, considering that the steel sheet was elongated along the longitudinal direction during rolling, as shown in previous work [22]. The mini-tensile test was conducted using the Instron 5948 R micro material testing machine with a chuck moving velocity of 0.1 mm/min. Strain was measured using a video-type extensometer and three experiments were conducted in each case to check the results repeatability. The morphology of the fracture surfaces was observed using scanning electron microscopy (SEM, JSM-5610LV), operated at 20 kV.

3. Results and discussion

3.1. Microstructure

Fig. 2 shows microstructure of the Fe-25Cr-20Ni steel before and after cryorolling. A single phase austenite with homogeneous microstructure and obvious grain boundaries before deformation is observed, and the grain size is about $60\text{ }\mu\text{m}$, as seen in Fig. 2a and b. After 90% deformation in Fig. 2c, the grain boundaries become blurred and the grains are elongated, contributing to the fibrous structure formation. From the corresponding TEM image in Fig. 2d, it can be seen that the grains of austenitic stainless steel are almost completely broken after 90% deformation. The selected area electron diffraction pattern (SAED) of the samples after 90% deformation exhibits diffraction rings, indicating that the grains of austenitic stainless steel refine to the nanometer scale. The corresponding grain refinement mechanism and the mechanical properties of the samples after cryorolling were discussed in previous work [22].

Microstructure of the Fe-25Cr-20Ni steel after 90% cryorolling and 10 min annealing at different temperatures is shown in Fig. 3. With the increase of the annealing temperature, static recovery occurs, along with static recrystallization and grain growth, leading to the formation of equiaxed austenitic grains with clear boundaries. Based on Fig. 3, steel microstructure after annealing at $600\text{ }^{\circ}\text{C}$ remains fibrous (Fig. 3a) and the corresponding area electron diffraction (SAED) pattern of the samples shows diffraction rings (Fig. 3b), indicating that the austenitic grain size is still at the nanometer scale and the average grain size is about 35 nm. Thus, the cryorolled samples are at the stage of recovery when annealed at $600\text{ }^{\circ}\text{C}$. As the annealing temperature increases to $700\text{ }^{\circ}\text{C}$, most of the fibrous structures disappear and the subgrains with the size of about 80 nm are formed. In local areas, some dislocation cells or dislocation walls are present, as seen in Fig. 3c and d. This indicates that the cryorolled samples are still at the stage of recovery when annealed at $700\text{ }^{\circ}\text{C}$. With further increase of annealing temperature to $800\text{ }^{\circ}\text{C}$, the fibrous structures completely disappeared and a large number of small equiaxed recrystallized grains appeared, as seen in Fig. 3e. From the TEM image in Fig. 3f, the dislocation density

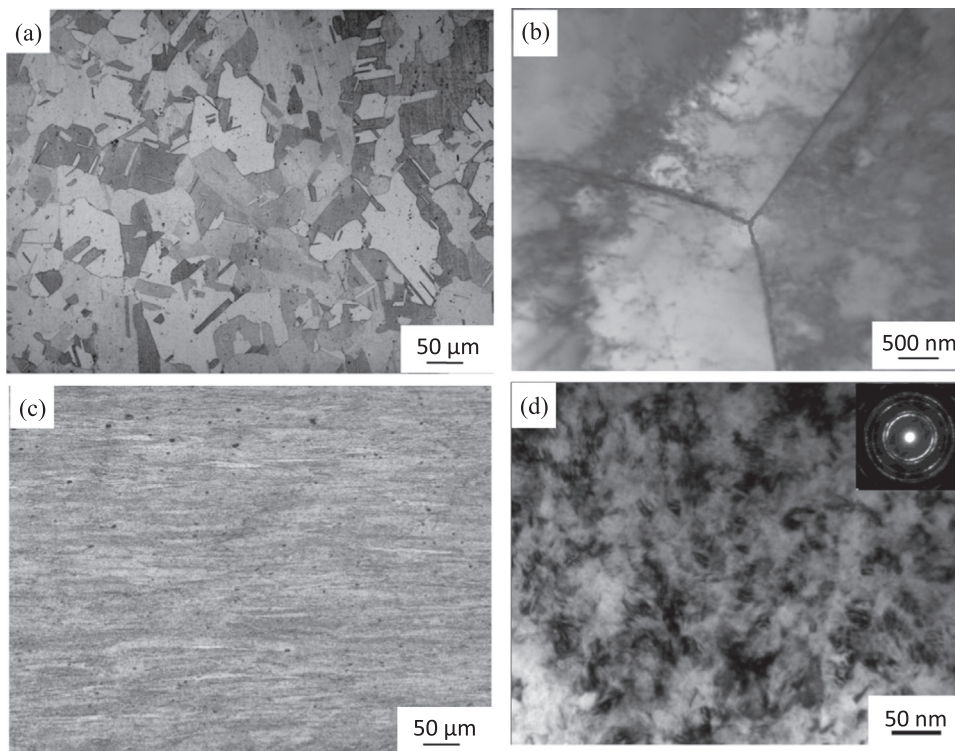


Fig. 2. Microstructure of the Fe-25Cr-20Ni steel before and after cryorolling: (a) and (b) original austenite structure; (c) and (d) after 90% deformation.

decreased significantly and the recrystallization completed. The grain boundaries of the recrystallized grains are flat and smooth, and the corresponding grain size is about 500 nm. When the annealing temperature is 1000 °C, the recrystallized grains grow to about 2 μm, as seen in Fig. 3g and f. Meanwhile, the SAED pattern of the samples changed from concentric rings to scattered spots with the annealing temperature increase. TEM images in Fig. 3f and h also indicate intra and inter-granular nano-precipitation of a $M_{23}C_6$ carbide and sigma-phase after annealing at 800 °C and 1000 °C [24]. The grain size of the precipitates increases with annealing temperature.

Etienne et al. [4] studied thermal stability of the 316 austenitic stainless steel with the grain size of 40 nm. Their results showed that the samples exhibited excellent thermal stability when the annealing temperature was lower than 700 °C, and the grain size was about 60 nm at 700 °C for 10 min annealing. When the annealing temperature exceeded 700 °C, the grain size increased to 380 nm (800 °C) and 780 nm (900 °C), respectively, which indicated that the recrystallization temperature of the nanocrystalline 316 austenitic stainless steel was 700 °C. In order to determine the recrystallization temperature of the nanocrystalline Fe-25Cr-20Ni steel, annealing temperatures of 730 °C, 750 °C and 770 °C were selected in this study. The corresponding microstructure is shown in Fig. 4. In Fig. 4a, a large amount of recrystallized grains with the size of about 100 nm are formed at 730 °C for 10 min annealing, and annealing twins are present in some recrystallized grains. As the annealing temperature increases to 750 °C, the grains grow to 150 nm with flat grain boundaries, and the width of the annealing twins increases, as seen in Fig. 4b. When the annealing temperature is 770 °C, the grain size increases to 200 nm and the annealing twins get wider, as seen in Fig. 4c. Thus, it can be deduced that the recrystallization temperature of the nanocrystalline Fe-25Cr-20Ni steel is about 730 °C.

It can be seen from Fig. 4 that the width of the annealing twins increases from 30 to 40 nm to 80–100 nm with annealing temperature. During the recrystallization, the interface migration decreases the interfacial energy and the existence of the stacking faults leads to the formation of flake twins in the semi-coherent matrix, which reduces the interfacial energy and results in the formation of the annealing twins

[25]. Kumar et al. [21] studied the microstructure of the brass processed by cryorolling followed by short annealing. They reported that the annealing twins were formed after 90% cryorolling and annealing at 300 °C for 20 min.

3.2. XRD analysis

The XRD patterns of the cryorolled Fe-25Cr-20Ni steel after 10 min annealing at different temperatures are shown in Fig. 5. As the annealing temperature increases from 500 °C to 1000 °C, the diffraction peaks become sharper. The full width at half maximum (FWHM) of (111) austenitic stainless steel is 0.429 (500 °C), 0.410 (600 °C), 0.403 (700 °C), 0.310 (800 °C), 0.296 (900 °C) and 0.295 (1000 °C), respectively. The FWHM of the samples before and after cryorolling is 0.324 and 0.496, respectively [22].

The FWHM of the annealed Fe-25Cr-20Ni steel is less than the cryorolled, which indicates obvious sharpening of the diffraction peak. When the annealing temperature is below 700 °C, the FWHM reduces slightly with the annealing temperature, while the FWHM decreases quickly as the temperature exceeds 700 °C. The decrease of FWHM is mainly due to the release of internal stress and grain growth. These results are consistent with the findings in Etienne's work [4]. They reported that the FWHM of the peaks decreased when the annealing temperature increased. Behjati et al. [26] found a similar phenomenon in the Fe-18Cr-12Mn-0.25 N austenitic stainless steel.

Based on the XRD results, the dislocation density was calculated, as listed in Table 1. The dislocation density is $4.3 \times 10^{15} \text{ m}^{-2}$ after 90% cryorolling. When the annealing temperature is below 700 °C, the dislocation density is on the scale of 10^{15} m^{-2} and reduces to $1.4 \times 10^{14} \text{ m}^{-2}$ at 800 °C annealing. The dislocation density decreases to the 10^{13} m^{-2} scale with further increase in annealing temperature. The change of the dislocation density is similar with the Shakhova's results [13]. They found that rapid structural refinement at early deformation stages is accompanied by the increase in dislocation density and martensitic transformation during subsequent cold rolling leads to further increase in dislocation density.

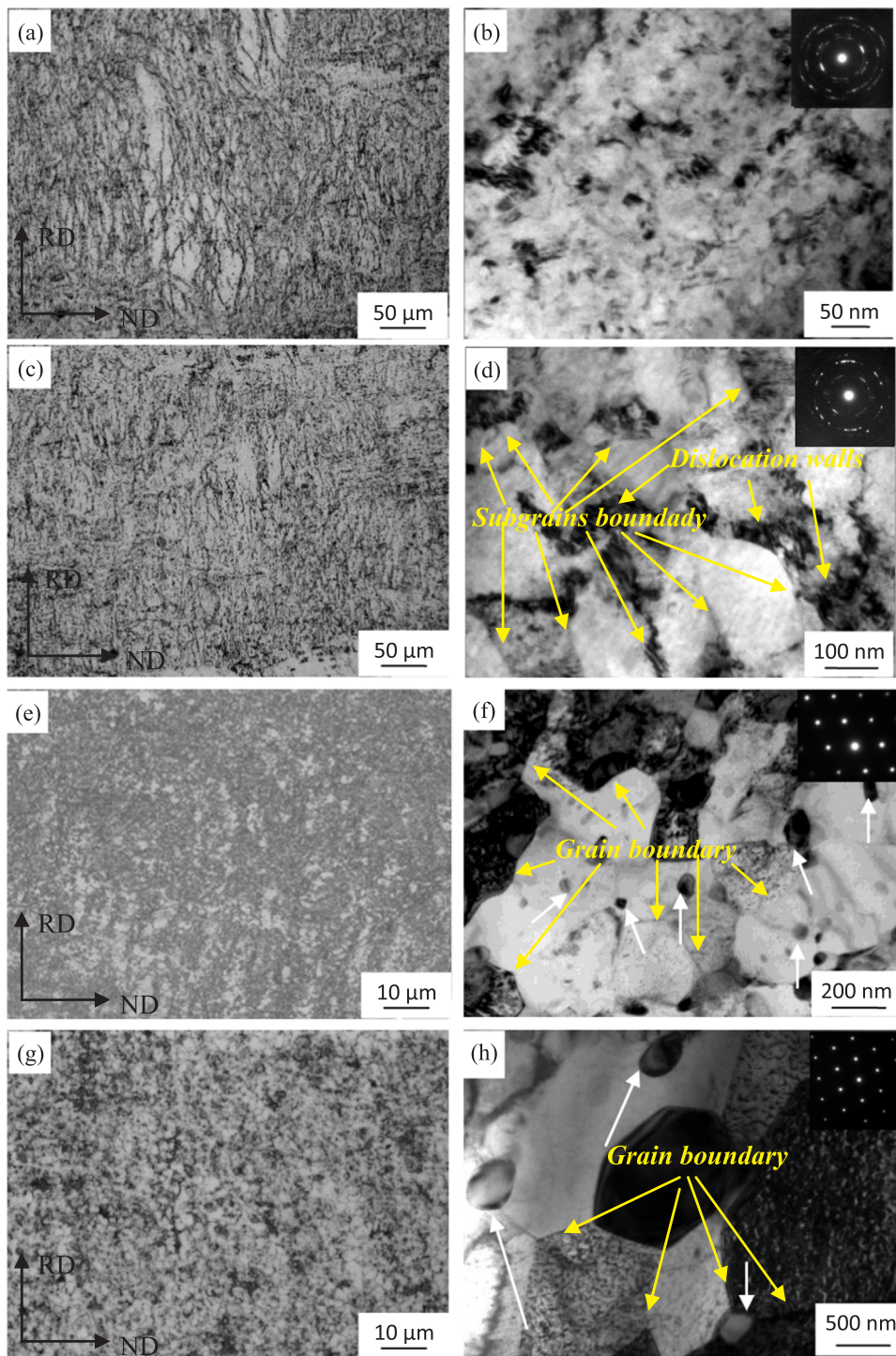


Fig. 3. Microstructures of the Fe-25Cr-20Ni steels after 90% cryorolling and 10 min annealing at different temperatures: (a) and (b) 600 °C; (c) and (d) 700 °C; (e) and (f) 800 °C; (g) and (h) 1000 °C. White arrows in (f) and (h) indicate precipitates inside grains and at grain boundaries.

3.3. Mechanical properties

Fig. 6 shows engineering stress-strain curves of the Fe-25Cr-20Ni steel annealed at different temperatures for 10 min. It can be seen that when the annealing temperature is below 700 °C, the strength of the annealed sample is higher than cryorolled, but the elongation is slightly lower than the cryorolled. When the annealing temperature is above 700 °C, the strength of the annealed sample is lower than of the cryorolled, but the elongation is significantly higher.

Mechanical properties of the annealed samples are shown in Fig. 7 and the data are listed in Table 1. After annealing at different temperatures, the strength and elongation change significantly. The

changes of the strength are the same as the microhardness, but contrary to the elongation. Previous results show that the tensile strength and the elongation of the Fe-25Cr-20Ni steel before cryorolling are 645 MPa and 40.8%, respectively, and the corresponding toughness is about 268 MPa. After 90% cryorolling, the yield strength and the tensile strength increase to 1502 MPa and 1560 MPa, respectively, while elongation and toughness reduce to 6.4% and 18 MPa [22]. The yield strength and the tensile strength increase further to 1597 MPa and 1685 MPa after annealing at 500 °C, while elongation and toughness are close to the cryorolled samples. When the annealing temperature rises to 600 °C, the tensile strength reduces, but the elongation and the toughness have no obvious change. When the annealing temperature is

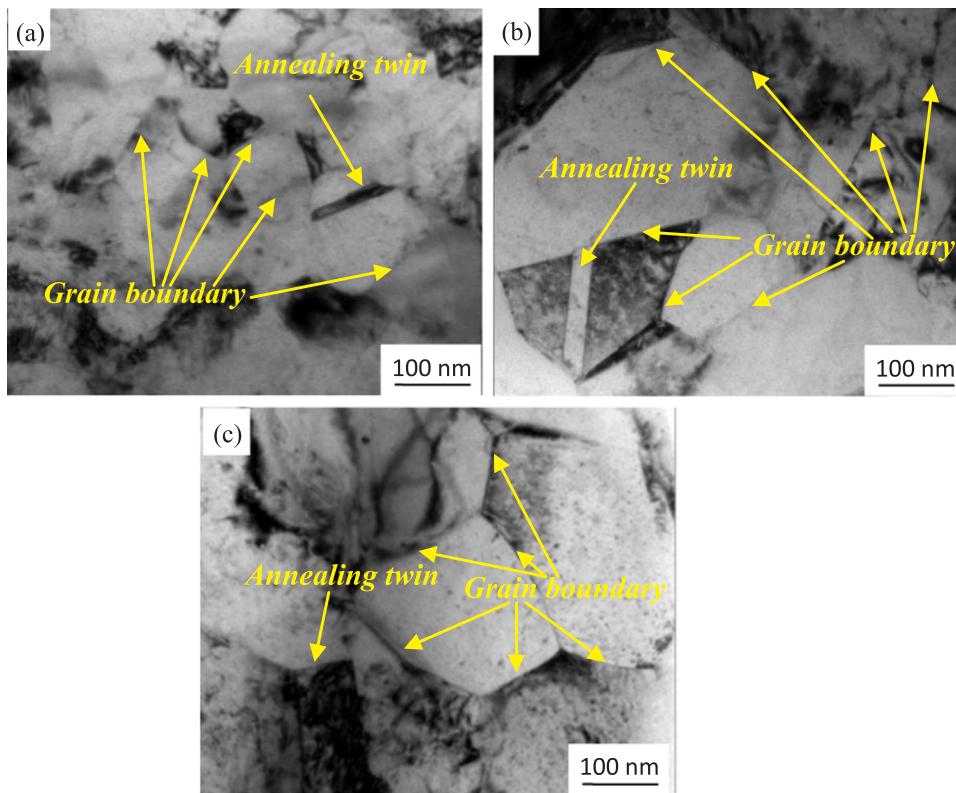


Fig. 4. Microstructure of the Fe-25Cr-20Ni steels after 90% cryorolling and annealed at: (a) 730 °C; (b) 750 °C; (c) 770 °C.

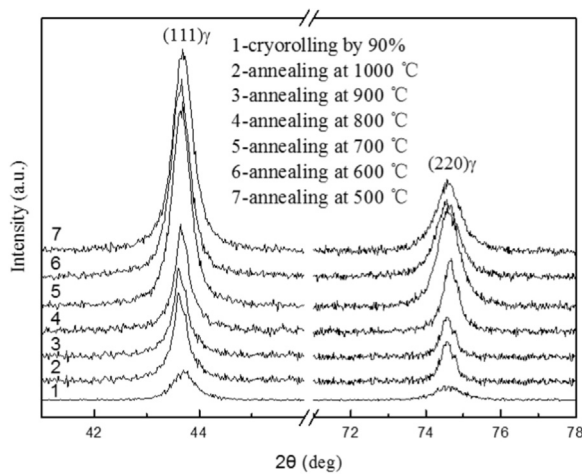


Fig. 5. Changes of XRD peak positions of the cryorolled Fe-25Cr-20Ni steels after 10 min annealing at different temperatures.

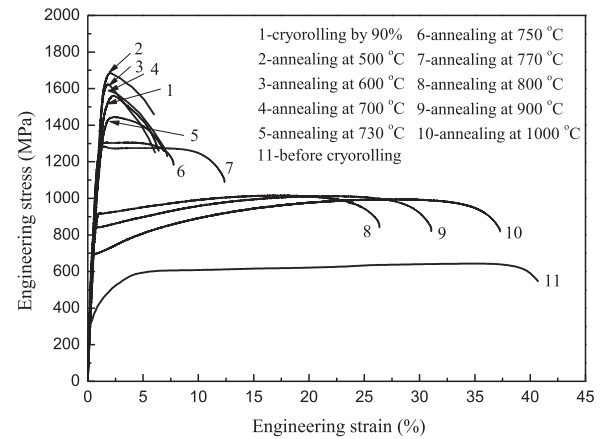


Fig. 6. Engineering stress-strain curves of the mini-tensile samples after 10 min annealing at different temperatures.

Table 1

Grain size, dislocation density and mechanical properties of austenitic stainless steels before and after cryorolling and subsequent annealing.

Sample	Grain size (nm)	Dislocation density (m^{-2})	Yield strength (MPa)	Tensile strength (MPa)	Elongation (%)	Toughness (MPa)
before cryorolling	60,000	—	305	645	40.8	268
after 90% cryorolling	20	4.3×10^{15}	1502	1560	6.4	18
annealed at 500 °C	—	1.8×10^{15}	1597	1685	6.0	20
annealed at 600 °C	35	1.2×10^{15}	1428	1623	6.1	26
annealed at 700 °C	80	1.0×10^{15}	1295	1598	7.2	36
annealed at 730 °C	100	—	1175	1446	7.7	68
annealed at 750 °C	150	—	1165	1305	8.6	85
annealed at 770 °C	200	—	1138	1274	12.3	150
annealed at 800 °C	500	1.4×10^{14}	915	1015	26.3	257
annealed at 900 °C	—	3.2×10^{13}	849	1012	31.0	296
annealed at 1000 °C	2000	2.5×10^{13}	693	994	37.3	341

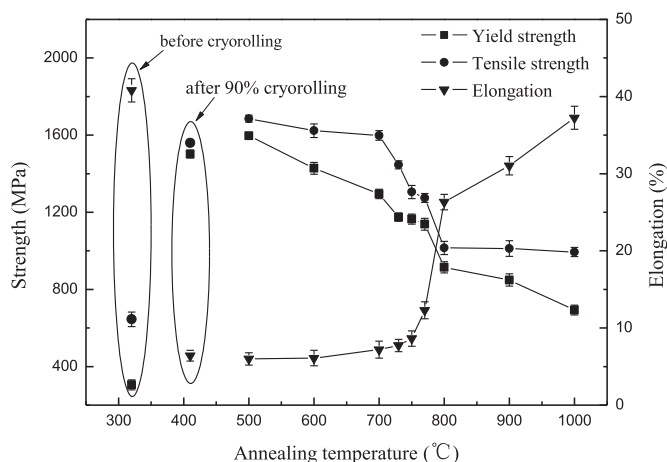


Fig. 7. Mechanical properties of the cryorolled Fe-25Cr-20Ni steels after 10 min annealing at different temperatures.

800 °C, the yield strength and the tensile strength decrease to 915 MPa and 1015 MPa, respectively, which is 3 and 1.6 times of the Fe-25Cr-20Ni steel without cryorolling. The elongation and toughness increase to 26.3% and 257 MPa, which are much higher than for the samples annealed at 500–700 °C, but close to the samples without cryorolling. By further increasing annealing temperature to 1000 °C, yield and tensile strengths decline to 693 MPa and 994 MPa, respectively, which is 2.3 and 1.5 times of the sample without cryorolling. The elongation rises to 37.3%, which is close to the sample without cryorolling (40.8%). The toughness increases to 341 MPa, which is 18.9 and 1.3 times of the samples after 90% cryorolling and without cryorolling, respectively.

TEM characterization of the samples subjected to 1000 °C annealing has shown the formation of fully recrystallized and coarse grains, which causes reduction in strength and increase in elongation. Thus, it can be seen that excellent comprehensive mechanical properties can be obtained at the annealing temperature above 800 °C. When the annealing temperature increases to 1000 °C, the grain size of the austenite stainless steel is only about 2 μm . The strength and the elongation are greatly improved.

Fig. 8 shows microhardness of the cryorolled Fe-25Cr-20Ni steel samples after 10 min at different temperatures. When the annealing temperature is 500 °C and 600 °C, the microhardness is 549 HV and 534 HV, respectively, which is higher than for the cryorolled samples at about 520 HV [22]. This may be attributed to the Cottrell atmosphere formed in the process of cryorolling, and the strain aging during subsequent heat treatment due to the Cottrell atmosphere making the dislocations movement much harder, thus the microhardness increased with the strength. These results are consistent with the findings in

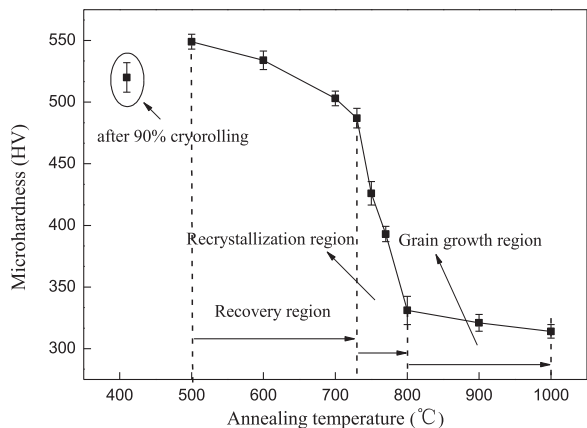


Fig. 8. Relationship between the microhardness and the annealing temperature.

reference [27]. M. Eskandari et al. [9] studied the effect of strain-induced martensite on the formation of nanocrystalline 316L stainless steel after cold rolling and annealing. They also found that the hardness followed a trend of initial rise followed by a fall, and stated that increased hardness was related to the production of the nano-grained structure, while decreased hardness was due to the grain growth. As the annealing temperature increases to 700 °C, the microhardness is 503 HV, which is lower than the cryorolled samples. The microhardness decreases mainly due to the full release of the strain aging and the reduction of dislocation density with the annealing temperature. However, large amounts of subgrains with the grain size of about 100 nm are formed (Fig. 3d), and the microhardness increases as a result of grain refinement. Thus, under the combined effects of the above reasons, the microhardness slowly declines. When the annealing temperature increases to 730 °C, 750 °C and 770 °C, the microhardness is 485 HV, 426 HV and 392 HV, respectively. At the early stage of recrystallization, the recrystallized grain size is at the nano-level, and the dislocation density is reduced compared to the recovery stage, leading to the slow decrease of the microhardness. The degree of recrystallization improves with annealing temperature and the dislocation density further reduces, thus, the microhardness declines significantly. When the annealing temperature is 800 °C, the microhardness is about 331 HV. When the annealing temperature increases to 900 °C and 1000 °C, the microhardness is 321 HV and 314 HV, respectively.

The microhardness decreases with the annealing temperature, and the trend is composed of the three distinct regions in Fig. 8. The first region is from 500 °C to 730 °C, where microhardness falls slowly, meaning no recrystallization, only recovery. Therefore, the first region is referred to as the “recovery region”. The second region is from 730 °C to 800 °C. This region is characterized by a large decrease in microhardness and is referred to as “recrystallization region”. A large number of new recrystallized grains without distortion form and dislocations disappear completely, leading to a sharp drop in microhardness. The third region is above 800 °C and is called “grain growth region” accompanied by a slight decrease in microhardness [28]. In this region, the recrystallized grains obviously grow, and equiaxed austenite structures with uniform, straight and clear grain boundaries eventually formed, so the microhardness gradually reduced. The change of the microhardness shows good agreement with Rao's results [29]. They reported that during recrystallization the hardness decreased rapidly, but during grain growth, it remained constant. Similar phenomenon was also observed in 6082 Al alloy after cryorolling and annealing by Kumar et al. [30]. Ren et al. [31] stated that the main factors influencing the microhardness are dislocation density, grain size and dislocation mobility. With the increase of the annealing temperature, the austenitic grains grow bigger, and the number of dislocations available for gliding is lower, and even completely disappeared. As a result, the microhardness of the Fe-25Cr-20Ni steel decreases tremendously.

3.4. Fractography analysis

Fig. 9a shows the fracture surface of the original austenitic stainless steel, which is typical ductile fracture. Many large and deep dimples with the average size of about 8 μm can be found. After 90% cryorolling, the sample fracture surface transforms from typical ductile to a mixture of cleavage and ductile fracture, as shown in Fig. 9b. The fracture surfaces morphology of the 90% cryorolled Fe-25Cr-20Ni steel after 10 min annealing is shown in Fig. 9c-h. At 500 °C annealing, the tensile fracture is flat and mixed with a few small and shallow dimples, as seen in Fig. 9c, indicating a mixture of quasi-cleavage and ductile fracture, which are similar to the cryorolled sample [22]. When the annealing temperature is 600 °C, the sample fracture surface is smooth and the tear ridges are observed in some regions. Meanwhile, a small amount of the dimples can be found in Fig. 9d. As the annealing temperature rises to 700 °C, the number and the size of the dimples

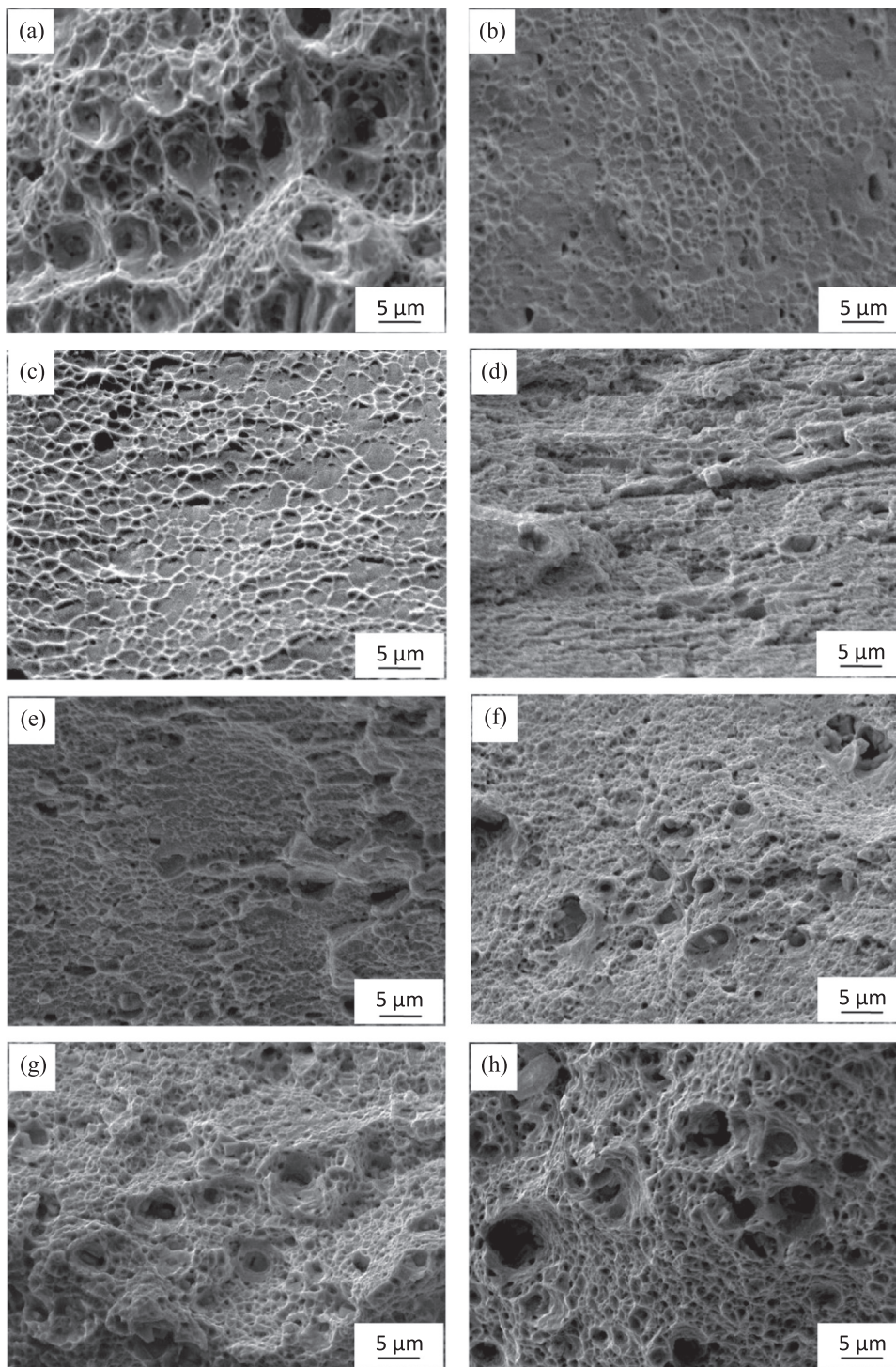


Fig. 9. Fracture surface morphology of the Fe-25Cr-20Ni steels: (a) original austenite structure; (b) after 90% cryorolling; the cryorolled Fe-25Cr-20Ni steels after 10 min annealed at: (c) 500 °C; (d) 600 °C; (e) 700 °C; (f) 800 °C; (g) 900 °C and (h) 1000 °C.

increase, as seen in Fig. 9e. When the annealing temperature increases to 800 °C, large and deep dimples with an average size of about 4 μm can be found in Fig. 9f, which is typical ductile fracture. By further increasing the annealing temperature to 900 °C and 1000 °C, the number of the dimples rises and the size of the dimples increases to 5 μm and 7 μm, respectively, found in Fig. 9g and h. This indicates that annealed specimens exhibit improved ductility with the annealing temperature increase. Therefore, the elongation of the samples sharply increases from 6% annealed at 500 °C to 37.3% annealed at 1000 °C, and the fracture morphology transforms from a mixture of quasi-cleavage and ductile fracture to ductile one. Baghbadorani et al. [32] stated that the fracture mode in the cold rolled sample was brittle with

cleavage facet-type morphology, and further annealing resulted in the formation of dimples and the dimple size increased with the holding time, as a result of increase in ductility of the samples. Meanwhile, the change of the fracture morphology in the present work shows good agreement with Kumar's results [21]. They stated that the samples after 90% cryorolling showed almost brittle type fracture with a limited number of smaller size dimples. The annealed samples exhibited an improved ductility with the increase in the annealing temperature due to recrystallization. Meanwhile, with the increase of the annealing temperature, the austenitic grains grew bigger, as seen in Fig. 9e-h. As a result, the elongation of the samples sharply increased with the annealing temperature.

4. Conclusions

In the present study, annealing effects on microstructure and mechanical properties of the cryorolled Fe-25Cr-20Ni steel were systematically characterized and analyzed. The results are as follows:

1. The ultrafine-grained Fe-25Cr-20Ni steel is successfully prepared by cryorolling and subsequent annealing. Excellent comprehensive mechanical properties can be obtained when the annealing temperature is higher than 800 °C with the holding time of 10 min. After annealing, the strength increases significantly, meanwhile the elongation and toughness are quite close to that of the original undeformed sample.
2. The recrystallization temperature of the cryorolled Fe-25Cr-20Ni steel is about 730 °C. With the increase of annealing temperature, the austenitic grains are fully recrystallized and the grain size increasingly grows.
3. Tensile fracture morphology of the cryorolled Fe-25Cr-20Ni steel changes from a mixture of quasi-cleavage and ductile fracture (before annealing) to typical ductile fracture (after annealing).

Acknowledgements

This work was supported by the National Natural Science Foundation of China under grants Nos. 50801021 and 51201061, and by Program for Science, Technology Innovation Talents in Universities of the Henan Province (17HASTIT026), the Science and Technology Project of the Henan Province (152102210077), International Scientific and Technological Cooperation Project from Science and Technology Department of Henan Province (172102410032), Education Department of the Henan Province (16A430005) and the Science and Technology Innovation Team of the Henan University of Science and Technology (2015XTD006).

References

- [1] Y. Estrin, A. Vinogradov, Extreme grain refinement by severe plastic deformation: a wealth of challenging science, *Acta Mater.* 61 (2013) 782–817.
- [2] J.X. Huang, X.N. Ye, Z. Xu, Effect of cold rolling on microstructure and mechanical properties of AISI 301LN metastable austenitic stainless steels, *J. Iron Steel Res. Int.* 19 (2012) 59–63.
- [3] A. Hedayati, A. Najafizadeh, A. Kermanpur, F. Forouzan, The effect of cold rolling regime on microstructure and mechanical properties of AISI 304L stainless steel, *J. Mater. Process. Technol.* 210 (2010) 1017–1022.
- [4] A. Etienne, B. Radiguet, C. Genevois, J.M. Le Breton, R. Valiev, P. Pareige, Thermal stability of ultrafine-grained austenitic stainless steels, *Mater. Sci. Eng. A* 527 (2010) 5805–5810.
- [5] B. Mahato, S. Sharma, J.K. Sahu, Effect of cyclic thermal process on ultrafine grain formation in AISI 304L austenitic stainless steel, *Metall. Mater. Trans. A* 40 (2009) 3226–3234.
- [6] T. Maki, Formation of ultrafine-grained structures by various thermomechanical processing in steel. *Proc Workshop on New Generation Steel (NG STEEL'2001)*, Beijing: The Chinese Society for Metals, 2001, p. 27.
- [7] C.X. Huang, G. Yang, Y.L. Gao, S.D. Wu, Z.F. Zhang, Influence of processing temperature on the microstructures and tensile properties of 304L stainless steel by ECAP, *Mater. Sci. Eng. A* 485 (2008) 643–650.
- [8] Y.F. Shen, N. Jia, Y.D. Wang, X. Sun, L. Zuo, D. Raabe, Suppression of twinning and phase transformation in an ultrafine grained 2 GPa strong metastable austenitic steel: experiment and simulation, *Acta Mater.* 97 (2015) 305–315.
- [9] M. Eskandari, A. Najafizadeh, A. Kermanpur, Effect of strain-induced martensite on the formation of nanocrystalline 316L stainless steel after cold rolling and annealing, *Mater. Sci. Eng. A* 519 (2009) 46–50.
- [10] B. Roy, R. Kumar, J. Das, Effect of cryorolling on the microstructure and tensile properties of bulk nano-austenitic stainless steel, *Mater. Sci. Eng. A* 631 (2015) 241–247.
- [11] B.R. Kumar, D. Raabe, Tensile deformation characteristics of bulk ultrafine-grained austenitic stainless steel produced by thermal cycling, *Scr. Mater.* 66 (2012) 634–637.
- [12] Y.F. Shen, X.M. Zhao, X. Sun, Y.D. Wang, L. Zuo, Ultrahigh strength of ultrafine grained austenitic stainless steel induced by accumulative rolling and annealing, *Scr. Mater.* (2014), <http://dx.doi.org/10.1016/j.scriptamat.2014.05.001>.
- [13] I. Shakhova, V. Dudko, A. Belyakov, K. Tsuzaki, R. Kaibyshev, Effect of large strain cold rolling and subsequent annealing on microstructure and mechanical properties of an austenitic stainless steel, *Mater. Sci. Eng. A* 545 (2012) 176–186.
- [14] Y.Q. Ma, J.E. Jin, Y.K. Lee, Repetitive thermomechanical process to produce nanocrystalline in a metastable austenitic steel, *Scr. Mater.* 52 (2005) 1311–1315.
- [15] H.B. Wu, F.J. Wu, S.W. Yang, D. Tang, The formation mechanism of austenite structure with micro/sub-micrometer bimodal grain size distribution, *Acta Metall. Sin.* 50 (2014) 269–274.
- [16] H.W. Huang, Z.B. Wang, J. Lu, K. Lu, Fatigue behaviors of AISI 316L stainless steel with a gradient nanostructured surface layer, *Acta Mater.* 87 (2015) 150–160.
- [17] Y.M. Wang, M.W. Chen, F.H. Zhou, E. Ma, High tensile ductility in a nanostructured metal, *Nature* 419 (2002) 912–915.
- [18] S.K. Panigrahi, R. Jayaganthan, Development of ultrafine grained Al-Mg-Si alloy with enhanced strength and ductility, *J. Alloy. Compd.* 470 (2009) 285–288.
- [19] Y.B. Lee, D.H. Shin, K.T. Park, W.J. Nam, Effect of annealing temperature on microstructures and mechanical properties of a 5083 Al alloy deformed at cryogenic temperature, *Scr. Mater.* 51 (2004) 355–359.
- [20] V.S. Sarma, K. Sivaprasad, D. Sturm, M. Heilmair, Microstructure and mechanical properties of ultra fine grained Cu-Zn and Cu-Al alloys produced by cryorolling and annealing, *Mater. Sci. Eng. A* 489 (2008) 253–258.
- [21] R. Kumar, S.M. Dasharath, P.C. Kang, C.C. Koch, S. Mula, Enhancement of mechanical properties of low stacking fault energy brass processed by cryorolling followed by short-annealing, *Mater. Des.* 67 (2015) 637–643.
- [22] Y. Xiong, T.T. He, J.B. Wang, Y. Lu, L.F. Chen, F.Z. Ren, Y.L. Liu, A.A. Volinsky, Cryorolling effect on microstructure and mechanical properties of Fe-25Cr-20Ni austenitic stainless steel, *Mater. Des.* 88 (2015) 398–405.
- [23] G.K. Williamson, W.H. Hall, X-ray line broadening from filed aluminium and wolfram, *Acta Metall.* 1 (1953) 22–31.
- [24] K. Ladislav, S. Stefan, K. Stjepan, Transformation of austenite during isothermal annealing at 600–900 °C for heat-resistant stainless steel, *J. Alloy. Compd.* 567 (2013) 59–64.
- [25] T.G. Liu, S. Xia, H. Li, B.X. Zhou, Q. Bai, Effect of the pre-existing carbides on the grain boundary network during grain boundary engineering in a nickel based alloy, *Mater. Charact.* 91 (2014) 89–100.
- [26] P. Behjati, A. Kermanpur, A. Najafizadeh, Effect of annealing temperature on nano-ultrafine grain of Ni-free austenitic stainless steel, *Mater. Sci. Eng. A* 592 (2014) 77–82.
- [27] T. Juuti, L.P. Karjalainen, R. Ruoppa, T. Taulavuori, Static strain ageing in some austenitic stainless steels, *Mater. Sci. Forum* 638–642 (2010) 3278–3283.
- [28] Z.J. Zheng, J.W. Liu, Y. Gao, Achieving high strength and high ductility in 304 stainless steel through bimodal microstructure prepared by post-ECAP annealing, *Mater. Sci. Eng. A* (2016), <http://dx.doi.org/10.1016/j.msea.2016.11.004>.
- [29] P.N. Rao, D. Singh, R. Jayaganthan, Effect of annealing on microstructure and mechanical properties of Al 6061 alloy processed by cryorolling, *Mater. Sci. Technol.* 29 (2013) 76–82.
- [30] N. Kumar, P.N. Rao, R. Jayaganthan, H.G. Brokmeier, Effect of cryorolling and annealing on recovery, recrystallisation, grain growth and their influence on mechanical and corrosion behaviour of 6082 Al alloy, *Mater. Chem. Phys.* 165 (2015) 177–187.
- [31] F.Z. Ren, S.Y. Zhao, W.H. Li, B.H. Tian, L.T. Yin, A.A. Volinsky, Theoretical explanation of Ag/Cu and Cu/Ni nanoscale multilayers softening, *Mater. Lett.* 65 (2011) 119–121.
- [32] H.S. Baghbadorani, A. Kermanpur, A. Najafizadeh, P. Behjati, A. Rezaee, M. Moallemi, An investigation on microstructure and mechanical properties of a Nb-microalloyed nano-ultrafine grained 201 austenitic stainless steel, *Mater. Sci. Eng. A* 636 (2015) 593–599.